

Characterization of Structure and Stability of Long Telomeric DNA G-Quadruplexes

Hai-Qing Yu,[†] Daisuke Miyoshi,[†] and Naoki Sugimoto^{*,†,‡}

Contribution from the Frontier Institute for Biomolecular Engineering Research (FIBER) and Department of Chemistry, Faculty of Science and Engineering, Konan University, 8-9-1 Okamoto, Higashinada-ku, Kobe 658-8501, Japan

Received June 27, 2006; E-mail: sugimoto@konan-u.ac.jp

Abstract: In the current study, we used a combination of gel electrophoresis, circular dichroism, and UV melting analysis to investigate the structure and stability of G-quadruplexes formed by long telomeric DNAs from *Oxytricha* and human, where the length of the repeat (n) = 4 to 12. We found that the *Oxytricha* telomeric DNAs, which have the sequence (TTTTGGGG) $_n$, folded into intramolecular and intermolecular G-quadruplexes depending on the ionic conditions, whereas human telomeric DNAs, which have the sequence (TTAGGG) $_n$, formed only intramolecular G-quadruplexes in all the tested conditions. We further estimated the thermodynamic parameters of the intramolecular G-quadruplex. We found that thermodynamic stabilities of G-quadruplex structures of long telomeric DNAs (n = 5 to 12) are mostly independent of sequence length, although telomeric DNAs are more stable when n = 4 than when n ≥ 5. Most importantly, when n is a multiple of four, the change in enthalpy and entropy for G-quadruplex formation increased gradually, demonstrating that the individual G-quadruplex units are composed of four repeats and that the individual units do not interact. Therefore, we propose that the G-quadruplexes formed by long telomeric DNAs (n ≥ 8) are bead-on-a-string structures in which the G-quadruplex units are connected by one TTTT (*Oxytricha*) or TTA (human) linker. These results should be useful for understanding the structure and function of telomeres and for developing improved therapeutic agents targeting telomeric DNAs.

Introduction

Telomeres, which are present on the ends of eukaryotic chromosomes in many species including vertebrates, *Saccharomyces cerevisiae*, *Tetrahymena*, and *Oxytricha nova*, are composed of tandem repeats of guanine-rich (G-rich) sequences.¹ Since the discovery of a strong association between telomere length and cellular aging,^{2,3} telomere research has been the focus of studies on cellular senescence and immortalization. In most organisms, the G-rich strand extends beyond the DNA duplex of the telomere to form a single-stranded 3'-overhang.⁴⁻⁶ In human somatic cells, the telomere is typically 5–8 kb in length with a single-strand 3'-overhang of 200 ± 75 bases.⁷

The G-rich strand can fold into a G-quadruplex with cyclic Hoogsteen base pairs of four guanine bases (G-quartets; Figure 1A).⁸ These DNA G-quadruplexes are of interest because they are possible targets for telomerase inhibition and may have other

physiological roles.⁹⁻¹¹ The structures and stabilities of G-quadruplexes are known to be dependent on the presence and concentrations of monovalent cations¹²⁻¹⁷ because the cations can coordinate the carbonyl oxygen of the guanine and promote stacking interactions of the G-quartets.¹⁸ For example, the sequence (GGGGTTTTGGGG)₂ folds into a single G-quadruplex structure in the presence of Na⁺, whereas it folds into at least two structures in the presence of K⁺.¹⁹ Another good example for demonstrating the importance of cations is the sequence AGGG(TTAGGG)₃, which folds into an intramolecular antiparallel G-quadruplex structure with two lateral loops and one diagonal loop in the presence of Na⁺ but into a distinct intramolecular parallel propeller G-quadruplex with three extra loops in the presence of K⁺.²⁰

[†] FIBER.

[‡] Department of Chemistry, Faculty of Science and Engineering.

- (1) Zakian, V. A. *Science* **1995**, *270*, 1601–1607.
- (2) Allsopp, R. C.; Vaziri, H.; Patterson, C.; Goldstein, S.; Younglai, E. V.; Futcher, A. B.; Greider, C. W.; Harley, C. B. *Proc. Natl. Acad. Sci. U.S.A.* **1992**, *89*, 10114–10118.
- (3) Vaziri, H.; Benchimol, S. *Curr. Biol.* **1998**, *8*, 279–282.
- (4) Klobutcher, L. A.; Swanton, M. T.; Donini, P.; Prescott, D. M. *Proc. Natl. Acad. Sci. U.S.A.* **1981**, *78*, 3015–3019.
- (5) Henderson, E. R.; Blackburn, E. H. *Mol. Cell Biol.* **1989**, *9*, 345–348.
- (6) McElligott, R.; Wellinger, R. J. *EMBO J.* **1997**, *16*, 3705–3714.
- (7) Wright, W. E.; Valere, M. T.; Kenneth, E. H.; Stephen, D. L.; Jerry, W. S. *Genes Dev.* **1997**, *11*, 2801–2809.
- (8) Williamson, J. R.; Raghuraman, M. K.; Cech, T. R. *Cell* **1989**, *59*, 871–880.
- (9) Sun, D.; Thompson, B.; Cathers, B. E.; Salazar, M.; Kerwin, S. M.; Trent, J. O.; Jenkins, T. C.; Neidle, S.; Hurley, L. H. *J. Med. Chem.* **1997**, *40*, 2113–2116.
- (10) Kerwin, S. M. *Curr. Pharm. Des.* **2000**, *6*, 441–471.
- (11) Baker, E. S.; Lee, J. T.; Sessler, J. L.; Bowers, M. T. *J. Am. Chem. Soc.* **2006**, *128*, 2641–2648.
- (12) Hardin, C. C.; Henderson, E.; Watson, T.; Prosser, J. K. *Biochemistry* **1991**, *30*, 4460–4472.
- (13) Hardin, C. C.; Watson, T.; Corregan, M.; Bailey, C. *Biochemistry* **1992**, *31*, 833–841.
- (14) Ross, W. S.; Hardin, C. C. *J. Am. Chem. Soc.* **1994**, *116*, 6070–6080.
- (15) Miura, T.; Benevides, J. M.; Thomas, G. J., Jr. *J. Mol. Biol.* **1995**, *248*, 233–238.
- (16) Hud, N. V.; Smith, F. W.; Anet, F. A.; Feigon, J. *Biochemistry* **1996**, *35*, 15383–15390.
- (17) Hardin, C. C.; Corregan, M. J.; Lieberman, D. V.; Brown, B. A. *Biochemistry* **1997**, *36*, 15428–15450.
- (18) Sket, P.; CČrnugelj, M.; Plavec, J. *Nucleic Acids Res.* **2005**, *33*, 3691–3697.
- (19) Črnugelj, M.; Hud, N. V.; Plavec, J. *J. Mol. Biol.* **2002**, *320*, 911–924.

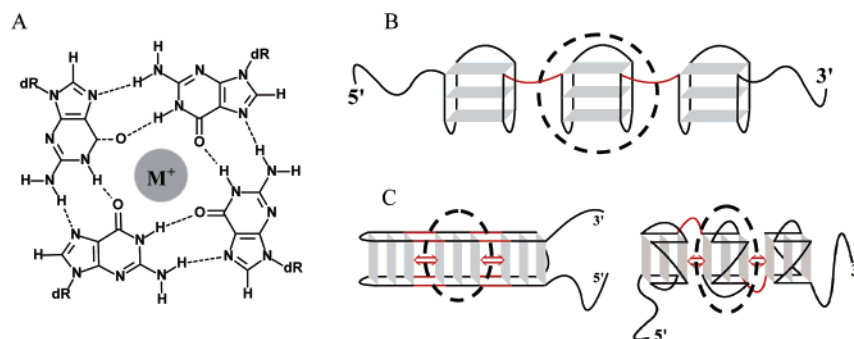


Figure 1. (A) Chemical structure of a G-quartet. M^+ is a metal ion. (B) Schematic illustration of the intramolecular bead-on-a-string structure of long telomeric DNAs. In this structure, two G-quadruplex units are connected by one linker (red lines) without a stacking interaction between the units. The structure in the dashed circle indicates the G-quadruplex unit. (C) Schematic illustrations of the intramolecular stacking structures of long telomeric DNAs. Left, two G-quadruplex units are connected by four linkers (red lines), and every G-quadruplex unit stacks on the other one (the stacking interaction is shown with red arrows). Right, two G-quadruplex units are connected by one linker (red lines), and every G-quadruplex unit stacks on the other one (the stacking interaction is shown with red arrows). The structures in the dashed circles indicate the G-quadruplex units.

There are also numerous studies on the thermodynamic or kinetic properties of G-quadruplex formation,^{21–25} but most of these studies have been carried out on short telomeric DNAs whose number of repeats is not more than four. Also, there is little direct evidence for the properties of long telomeric DNAs; these have instead been estimated on the basis of numerous studies of short telomeric DNAs. Therefore, structural and thermodynamic investigations are needed to reveal the actual structure of long telomeric DNAs. Such studies will establish whether the numerous previous studies of short telomeric DNAs are useful for predicting the structures of long telomeric DNAs. The properties of long telomeric DNAs should also be useful for the effective design of drugs and ligands targeting the telomere.

In the current study, we investigated the structural and thermodynamic properties of G-quadruplexes of long telomeric DNAs derived from *Oxytricha* and humans in the presence of K^+ or Na^+ . The *Oxytricha* and human telomeric DNAs used in this study were $(TTTGGGG)_n$ and $(TTAGGG)_n$, respectively, where n , the number of repeats, was 4–12. We studied the G-quadruplex structures formed by the long telomeric DNAs and their thermodynamic parameters using nondenaturing polyacrylamide gel electrophoresis (PAGE), circular dichroism (CD) spectroscopy, and thermal melting analysis as followed by UV spectroscopy. The results of nondenaturing PAGE and CD showed that structural polymorphism of the long telomeric DNAs depends on their sequence and length as well as the ionic conditions. For example, *Oxytricha* telomeric DNAs were able to fold into intramolecular and intermolecular G-quadruplexes depending on the ionic conditions, although we confirmed that the intramolecular G-quadruplex is more stable under near-physiological ionic conditions. In contrast, the human telomeric DNAs formed only an intramolecular G-quadruplex in all the conditions tested. Furthermore, thermodynamic analysis of the intramolecular G-quadruplexes formed by *Oxytricha* or human telomeric DNAs indicated that the stabilities of the G-quadruplexes folded by long telomeric DNAs are independent of sequence length, although telomeric DNAs with four repeats

($n = 4$) are more stable than longer ones ($n \geq 5$). Also, the G-quadruplex structure was affected by the flanking sequences on the ends of the main G-quadruplex structure in all tested conditions. Most importantly, the enthalpy and entropy changes for the formation of intramolecular G-quadruplexes by telomeric DNAs, where n was a multiple of 4, suggested that the G-quadruplex unit (dashed circles in Figure 1) of long telomeric DNAs was a bead-on-a-string (Figure 1B) rather than a stacked structure (Figure 1C). These results should help advance telomere science and aid in the development of new G-quadruplex-based therapeutic agents.

Experimental Section

Materials. Oligodeoxynucleotides used in this study were purchased from Hokkaido System Science Co., Ltd. (Hokkaido, Japan) after purification by HPLC. Single-strand concentrations of the DNA oligodeoxynucleotides were determined by measuring the absorbance at 260 nm and high temperature using a UV-1700 spectrometer (Shimadzu Co., Ltd., Kyoto, Japan) connected to a Shimadzu TMSPC-8 thermoprogrammer (Shimadzu). Single-strand extinction coefficients were calculated from mononucleotide and dinucleotide data using the nearest-neighbor approximation.²⁶ All chemical reagents were of reagent grade from Wako Pure Chemical Co., Ltd. (Osaka, Japan) and used without further purification.

Nondenaturing PAGE. Samples (1 μ L of 10 μ M) were separated by nondenaturing PAGE on 20% acrylamide (19:1 acrylamide/bisacrylamide) gels at 5 V cm^{-1} and 4 $^{\circ}C$. Gels were stained with GelStar nucleic acid gel stain (Cambrex, Baltimore, MD) and imaged under UV illumination using FLS-5100 film (Fuji Photo Film Co., Ltd., Tokyo, Japan). All measurements were carried out in 50 mM Tris-HCl buffer (pH 7.0). Before measurements, the samples were annealed by heating to 90 $^{\circ}C$ for 10 min, cooled to 0 $^{\circ}C$ at 0.2 $^{\circ}C min^{-1}$, and incubated at 4 $^{\circ}C$ overnight.

CD Spectroscopy. CD spectroscopy is a highly sensitive method for determining the conformation of G-quadruplex structures. Antiparallel G-quadruplexes show positive and negative peaks around 295 and 265 nm, respectively, whereas parallel G-quadruplex structures shows positive and negative peaks around 260 and 240 nm, respectively.²⁷ In the current study, the CD spectra of DNA oligonucleotides were measured for 10 μ M DNA total strand concentration using a J-820 spectropolarimeter (JASCO Co., Ltd., Hachioji, Japan) with a 0.1-cm path length quartz cell at 4 $^{\circ}C$. The CD spectrum was obtained by

(20) Parkinson, G. N.; Lee, M. P. H.; Neidle, S. *Nature* **2002**, *417*, 876–880.

(21) Lu, M.; Guo, Q.; Kallenbach, N. R. *Biochemistry* **1992**, *31*, 2455–2459.

(22) Lu, M.; Guo, Q.; Kallenbach, N. R. *Biochemistry* **1993**, *32*, 598–601.

(23) Mergny, J. L.; Phan, A. T.; Lacroix, L. *FEBS Lett.* **1998**, *435*, 74–78.

(24) Phan, A. T.; Patel, D. J. *J. Am. Chem. Soc.* **2003**, *125*, 15021–15027.

(25) Mergny, J. L.; Cian, A. D.; Ghelab, A.; Saccà, B.; Lacroix, L. *Nucleic Acids Res.* **2005**, *33*, 81–94.

(26) Richard, E. G. *Handbook of Biochemistry and Molecular Biology*; CRC Press: Cleveland, OH, 1975.

(27) Miyoshi, D.; Matsumura, S.; Nakano, S.; Sugimoto, N. *J. Am. Chem. Soc.* **2004**, *126*, 165–169.

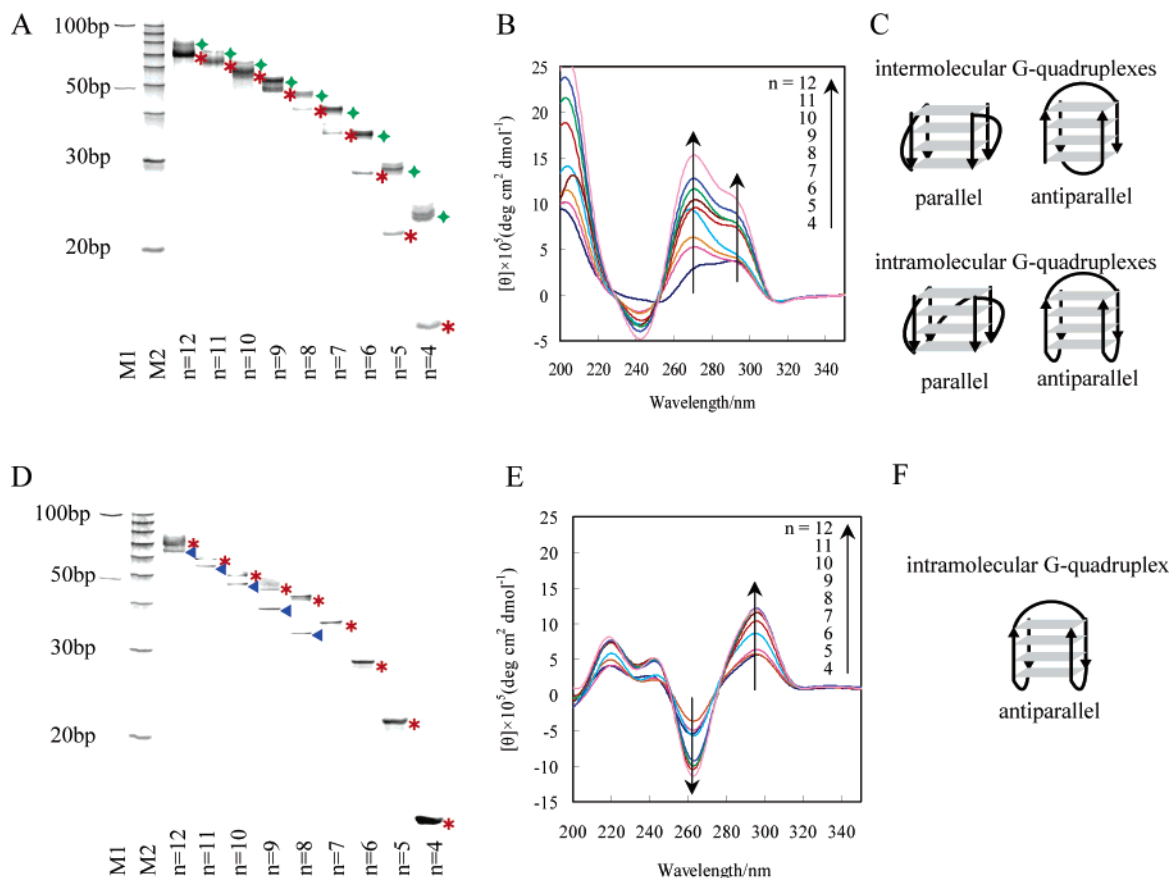


Figure 2. (A) Nondenaturing 20% PAGE of $(TTTTGGGG)_{n=4-12}$ in the presence of 100 mM K^+ at 4 °C (pH 7.0). Lane 1, 50-bp DNA standard; lane 2, 10-bp DNA standard. (B) CD spectra of $(TTTTGGGG)_{n=4-12}$ measured at 4 °C in 50 mM Tris-HCl (pH 7.0) containing 100 mM K^+ . The intensities of the CD spectra of the long telomeric DNAs generally increased with the repeat number. A recent conformational analysis of the G-quadruplex structures revealed that the CD spectra of an antiparallel G-quadruplex structure had a positive peak near 295 nm and a negative peak near 265 nm, whereas a parallel G-quadruplex structure had positive and negative peaks near 260 and 240 nm, respectively.^{26,27} (C) Schematic structures of the intermolecular and intramolecular G-quadruplex in the presence of K^+ . (D) Nondenaturing 20% PAGE of $(TTTTGGGG)_{n=4-12}$ in the presence of 100 mM Na^+ at 4 °C (pH 7.0). Lane 1, 50-bp DNA standard; lane 2, 10-bp DNA standard. (E) CD spectra of $(TTTTGGGG)_{n=4-12}$ measured at 4 °C in 50 mM Tris-HCl (pH 7.0) containing 100 mM Na^+ . The intensities of CD spectra of the long telomeric DNAs generally increased with the repeat number. (F) Schematic structure of the intramolecular G-quadruplex in the presence of Na^+ . In panels B and E, the number of repeats (n) is indicated as follows: 4, blue; 5, purplish red; 6, orange; 7, light blue; 8, red; 9, brown; 10, green; 11, dark blue; 12, pink.

taking the average of three scans made at 0.5-nm intervals from 200 to 350 nm. Before measurement, the DNA sample was heated at 90 °C for 10 min, gently cooled at 0.2 °C min^{-1} , and incubated at 4 °C overnight. The temperature of the cell holder was regulated by a PTC-348 temperature controller (JASCO), and the cuvette-holding chamber was flushed with a constant stream of dry N_2 gas to avoid water condensation on the cuvette exterior.

Thermodynamic Analysis. UV melting curves of G-quadruplexes were measured at 295 nm²³ using a UV-1700 spectrometer (Shimadzu). Before measurement, samples were heated at 90 °C for 10 min, gently cooled from 90 to 0 °C at 0.2 °C min^{-1} , and incubated at 4 °C overnight. The samples were then heated from 0 to 90 °C at 0.2 °C min^{-1} . The temperature of the cell holder was controlled by a TMSPC-8 temperature controller (Shimadzu), and water condensation on the cuvette exterior in the low-temperature range was avoided by flushing with a constant stream of dry N_2 gas. To calculate thermodynamic parameters, including the melting temperature (T_m), the enthalpy change (ΔH°), the entropy change (ΔS°), and the free energy change at 37 °C (ΔG_{37}°) for intramolecular G-quadruplex formation, the melting curves were fit²⁸ to the theoretical equation for an intramolecular association.

Results and Discussion

Structures of Long *Oxytricha* Telomeric DNAs. We carried out nondenaturing PAGE and CD experiments to investigate

the structures of *Oxytricha* telomeric DNAs in the presence of 100 mM K^+ . Figure 2A shows the results of nondenaturing PAGE for $(TTTTGGGG)_{n=4-12}$ in a buffer containing 100 mM KCl and 50 mM Tris-HCl (pH 7.0) at 4 °C. We observed two distinct bands with clearly different mobilities for each DNA. For $(TTTTGGGG)_4$, the lower band (labeled with a red asterisk in Figure 2A) migrated much faster than that of the 20-base pair duplex. This suggests that the lower band corresponds to an intramolecular G-quadruplex^{29,30} because an intermolecular G-quadruplex such as a dimer of 64 bases would migrate slower than the 20-base pair duplex of 40 bases. On the other hand, a dramatic decrease in the mobility of the slower band (labeled with a green star) indicates that the band corresponds to an intermolecular G-quadruplex as indicated by thermodynamic analysis (see “Thermodynamic Properties of the Long *Oxytricha* Telomeric DNAs”). Because all of the other sequences showed similar migration patterns, it appears that all of the samples fold into intramolecular and intermolecular G-quadruplexes.

(28) Markey, L. A.; Breslauer, K. J. *Biopolymers* **1987**, *26*, 1601–1620.

(29) Vorlíčková, M.; Chládková, J.; Kejnovská, I.; Fialová, M.; Kypr, J. *Nucleic Acids Res.* **2005**, *33*, 5851–5860.

(30) He, Y.; Neumann, R. D.; Panyutin, I. G. *Nucleic Acids Res.* **2004**, *32*, 5359–5367.

Figure 2B shows the CD spectra of the *Oxytricha* telomeric DNAs under the same conditions. The CD spectrum of each *Oxytricha* telomeric DNA has two positive peaks around 265 and 290 nm, indicating that these sequences form both parallel and antiparallel G-quadruplexes.³¹ Although short *Oxytricha* telomeric DNAs such as GGGGTTTTGGGG or GGGG-(TTTTGGGG)₃ are reported to form intermolecular or intramolecular antiparallel G-quadruplexes, respectively, in the presence of K⁺,^{32,33} the current results suggest that the longer *Oxytricha* telomeric DNAs ($n \geq 4$) fold into a mixture of parallel and antiparallel G-quadruplexes. On the other hand, the propeller G-quadruplex structure with extra loops enables the monomeric or dimeric G-quadruplex of human telomeric DNAs to form a parallel structure.^{20,24} On the basis of these results, it is possible that the parallel topologic structure may also be formed by *Oxytricha* telomeric DNAs in monomeric or dimeric G-quadruplexes as shown in Figure 2C.

We also studied the structures of the *Oxytricha* telomeric DNAs in the presence of Na⁺. We carried out nondenaturing PAGE of *Oxytricha* telomeric DNAs in a buffer containing 100 mM NaCl and 50 mM Tris-HCl (pH 7.0) at 4 °C (Figure 2D). We found that there was only one band (labeled with red asterisks) for the relatively shorter sequences ($n = 4-7$). In all of the samples, the band migrated at the position of the faster band observed in the presence of K⁺, indicating that it corresponds to an intramolecular G-quadruplex. The migration profiles of the longer sequences ($n = 8-12$) were more complicated than those of the shorter sequences. For these longer sequences, in addition to the band corresponding to the intramolecular structure (labeled with a red asterisk), there was another distinct band with a higher mobility (labeled with a blue triangle). Although further studies are required to determine the nature of the higher mobility band, it may be due to a more compact intramolecular structure. In the corresponding CD spectra (Figure 2E), all of the sequences have a single positive peak near 295 nm and a single negative peak near 260 nm, indicating that the *Oxytricha* telomeric DNAs ($n = 4-12$) form an antiparallel G-quadruplex structure in the presence of Na⁺. Na⁺ has been previously shown to induce the formation of antiparallel G-quadruplexes by short *Oxytricha* telomeric DNAs, namely, GGGTTTTGGG and GGGG-(TTTTGGGG)₃.³⁴⁻³⁷ The current results are consistent with these previous findings, indicating that all of the sequences form antiparallel G-quadruplexes in the presence of Na⁺ as depicted in Figure 2F.

Structures of Long Human Telomeric DNAs. We next examined the structures of human telomeric DNAs using nondenaturing PAGE and CD spectroscopy. Figure 3A shows the results of nondenaturing PAGE for the human telomeric sequence, (TTTAGG) _{$n=4-12$} , in a buffer containing 100 mM KCl and 50 mM Tris-HCl (pH 7.0) at 4 °C. In contrast to the *Oxytricha* DNAs, there was a single band for all of the human telomeric DNAs, and its migration indicated an intramolecular

structure. The CD spectra of the human telomeric DNAs in the same condition, however, showed two positive peaks near 290 and 260 nm, indicating a mixture of parallel and antiparallel G-quadruplexes (Figure 3B). Previous reports indicated a mixture of parallel and antiparallel G-quadruplexes for a short human telomeric DNA, AGGG(TTAGGG)₃.^{30,38} The parallel G-quadruplex structure of short human telomeric DNAs, such as TAGGGTTAGGGT or AGGG(TTAGGG)₃, was further shown to be a propeller G-quadruplex with extra loops,^{20,24} whereas the antiparallel G-quadruplex structure included lateral loops.³⁸ Because these antiparallel and parallel G-quadruplexes are intramolecular structures, the two appear to have similar molecular weights and global shapes. Therefore, they cannot be resolved by nondenaturing PAGE and appear as a single band. Our nondenaturing PAGE and CD results are consistent and indicate that the long human telomeric DNAs fold into a mixture of parallel and antiparallel G-quadruplexes in the presence of K⁺ as depicted in Figure 3C.

Figure 3D shows the nondenaturing PAGE image of human telomeric DNAs in a buffer containing 100 mM NaCl and 50 mM Tris-HCl (pH 7.0) at 4 °C. The results show that, in the presence of Na⁺, the human DNAs also appeared as single bands, and their migration indicated an intramolecular structure. Figure 3E shows the CD spectra of the human telomeric DNAs in the same condition. The CD spectra have a positive peak near 295 nm and a negative peak near 260 nm, demonstrating that the DNAs fold into antiparallel G-quadruplexes. These nondenaturing PAGE and CD results confirm that Na⁺ induces the formation of antiparallel G-quadruplex regardless of whether the telomeric sequence is short (e.g., AGGG(TTAGGG)₃),³⁹ or long ($n \geq 4$) (Figure 3F).

These PAGE and CD results reveal that long telomeric DNAs fold into different structures depending on the species, length, and ionic conditions. Importantly, we confirmed that the structure of *Oxytricha* and human telomeric DNAs is neither a random aggregate nor a higher order structure such as a G-wire.^{40,41} Moreover, we showed that the effect of monovalent cations on the G-quadruplex structure is equally important for long and short telomeric DNAs.^{20,24,32-39}

Thermodynamic Properties of the Long *Oxytricha* Telomeric DNAs. We investigated the thermodynamic properties of the G-quadruplex structures formed by the long *Oxytricha* telomeric DNAs by analyzing thermal melting curves generated from UV absorbance measurements at 295 nm.²³ Figure 4A shows the annealing and melting curves of (TTTTGGGG)₄ in a buffer containing 100 mM KCl and 50 mM Tris-HCl (pH 7.0). The hysteresis between the annealing and melting curves indicates that the folding of the *Oxytricha* sequence in the presence of K⁺ does not occur via a two-state transition. Rather, two distinct transitions were observed in the melting process, suggesting that at least two structures coexist in solution. Figure 4B shows the T_m values of the higher and lower temperature transitions (T_{mH} and T_{mL} , respectively) versus the concentration of (TTTTGGGG)₄. The T_{mH} values were independent of the DNA concentration, demonstrating that the structure unfolded

(31) Miyoshi, D.; Karimata, H.; Sugimoto, N. *Angew. Chem., Int. Ed.* **2005**, *44*, 3740-3744.

(32) Smith, F. W.; Feigon, J. *Biochemistry* **1993**, *32*, 8682-8692.

(33) Balagurumorthy, P.; Brahmachari, S. K. *Indian J. Biochem. Biophys.* **1995**, *32*, 385-390.

(34) Smith, F. W.; Lau, F. W.; Feigon, J. *Proc. Natl. Acad. Sci. U.S.A.* **1994**, *91*, 10546-10550.

(35) Strahan, G. D.; Keniry, M. A.; Shafer, R. H. *Biophys. J.* **1998**, *75*, 968-981.

(36) Keniry, M. A.; Strahan, G. D.; Owen, E. A.; Shafer, R. H. *Eur. J. Biochem.* **1995**, *233*, 631-643.

(37) Wang, Y.; Patel, D. J. *J. Mol. Biol.* **1995**, *251*, 76-94.

(38) Li, J.; Correia, J. J.; Wang, L.; Trent, J. O.; Chaires, J. B. *Nucleic Acids Res.* **2005**, *33*, 4649-4659.

(39) Wang, Y.; Peter, D. J. *Structure* **1993**, *1*, 263-282.

(40) Marsh, T. C.; Vesenska, J.; Henderson, E. *Nucleic Acid Res.* **1993**, *23*, 696-700.

(41) Miyoshi, D.; Nakao, A.; Sugimoto, N. *Nucleic Acid Res.* **2003**, *31*, 1156-1163.

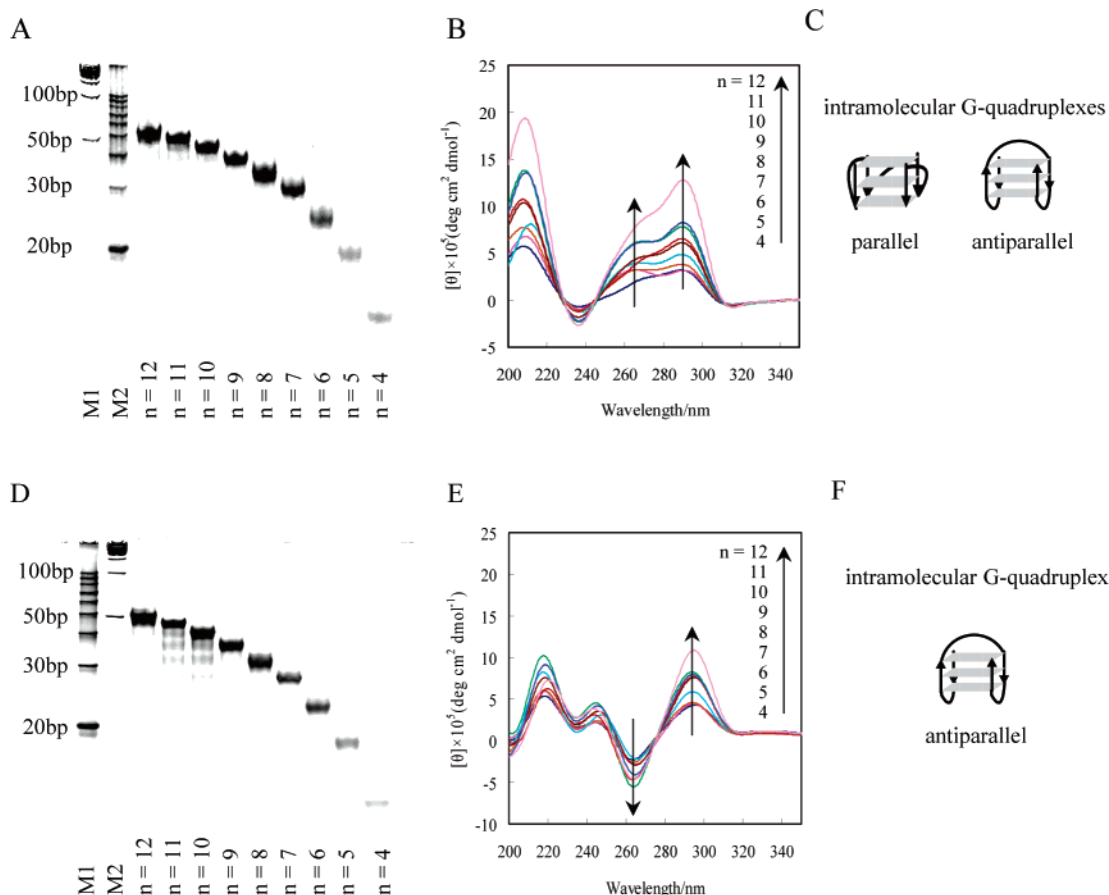


Figure 3. (A) Nondenaturing 20% PAGE of $(TTAGGG)_{n=4-12}$ in the presence of 100 mM K^+ at 4 °C (pH 7.0). Lane 1, 50-bp DNA standard; lane 2, 10-bp DNA standard. (B) CD spectra of $(TTAGGG)_{n=4-12}$ measured at 4 °C in 50 mM Tris-HCl (pH 7.0) containing 100 mM K^+ . The intensities of CD spectra of the long telomeric DNAs generally increased with the repeat number. (C) Schematic structures of the intramolecular G-quadruplex in the presence of K^+ . (D) Nondenaturing 20% PAGE of $(TTAGGG)_{n=4-12}$ in the presence of 100 mM Na^+ at 4 °C (pH 7.0). Lane 1, 10-bp DNA standard; lane 2, 50-bp DNA standard. (E) CD spectra of $(TTAGGG)_{n=4-12}$ measured at 4 °C in 50 mM Tris-HCl (pH 7.0) containing 100 mM Na^+ . The intensities of CD spectra of the long telomeric DNAs generally increased with the repeat number. (F) Schematic structure of the intramolecular G-quadruplex in the presence of Na^+ . In panels B and E, the number of repeats (n) is indicated as follows: 4, blue; 5, purplish red; 6, orange; 7, light blue; 8, red; 9, brown; 10, green; 11, dark blue; 12, pink.

at the higher temperature is an intramolecular G-quadruplex. On the other hand, the T_{mL} values increased with the DNA concentration, indicating that the structure unfolded at the lower temperature is an intermolecular G-quadruplex. These results show that the intramolecular G-quadruplex is more stable than the intermolecular G-quadruplex. The other *Oxytricha* telomeric DNAs, $(TTTTGGGG)_{n=5-12}$, behaved in a similar manner in the presence of K^+ (see Figures S1A and S1B for the melting curves and the plot of T_m versus the concentration of DNA). Comparison of the nondenaturing PAGE analyses for the *Oxytricha* telomeric DNAs (Figure 2A,B) and the UV-melting results shows that the intermolecular structure that unfolded at the lower temperature corresponds to the slower band, whereas the intramolecular structure unfolded at the higher temperature corresponds to the faster band.

We also evaluated the thermodynamic stability of the G-quadruplexes formed by *Oxytricha* telomeric DNAs in the presence of Na^+ . Figure 4C shows the annealing and melting curves for $(TTTTGGGG)_4$ in a buffer containing 100 mM NaCl and 50 mM Tris-HCl (pH 7.0) at 4 °C (see also Figure S1C for the melting curves for $(TTTTGGGG)_{n=5-12}$). In contrast to the melting curve in the presence of K^+ , the melting curve in the presence of Na^+ shows a single sigmoid shape. Although $(TTTTGGGG)_{n=8-12}$ folds into two intramolecular structures

as observed by nondenaturing PAGE (Figure 2C), the melting curves with a single sigmoid shape indicate that the thermodynamic stabilities of the two G-quadruplex structures are very similar. Furthermore, the T_m values were independent of the DNA concentration (Figure 4D for $(TTTTGGGG)_4$ and Figure S1D for $(TTTTGGGG)_{n=5-12}$), confirming the formation of intramolecular antiparallel G-quadruplexes by *Oxytricha* telomeric DNAs in the presence of Na^+ . These melting behaviors in the presence of K^+ or Na^+ are consistent with the structures determined by nondenaturing PAGE and CD (Figure 2C,D).

Using these melting curves, we further attempted to estimate the thermodynamic parameters for the formation of the G-quadruplex structures by *Oxytricha* telomeric DNAs. Although the non-two-state transition of *Oxytricha* telomeric DNAs makes it difficult to estimate the parameters in the presence of K^+ (Figures 4A and S1A), a hysteresis was not observed in the presence of Na^+ (Figures 4C and S1C), indicating that the formation of the intramolecular antiparallel G-quadruplex is in a two-state transition. Therefore, we calculated the values of ΔH° , ΔS° , and ΔG°_{37} by fitting the melting curves in the presence of Na^+ to the theoretical equation for an intramolecular association.²⁸

Figure 5 shows the ΔH° and ΔS° values for the antiparallel G-quadruplexes of $(TTTTGGGG)_{n=4-12}$ in the presence of 100

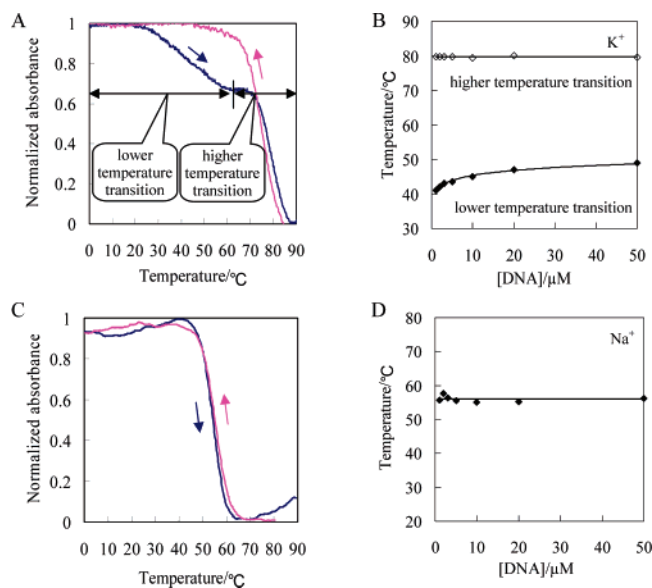


Figure 4. (A) Normalized thermal annealing (pink) and melting (blue) profiles recorded at 295 nm for (TTTTGGGG)₄ in 50 mM Tris-HCl (pH 7.0) containing 100 mM K⁺. (B) Plot of T_m vs concentration of (TTTTGGGG)₄ (1–50 μM strand concentration) in 50 mM Tris-HCl (pH 7.0) containing 100 mM K⁺. (C) Normalized thermal annealing (pink) and melting (blue) profile recorded at 295 nm for (TTTTGGGG)₄ in 50 mM Tris-HCl (pH 7.0) containing 100 mM Na⁺. (D) Plot of T_m vs concentration of (TTTTGGGG)₄ (1–50 μM strand concentration) in 50 mM Tris-HCl (pH 7.0) containing 100 mM Na⁺.

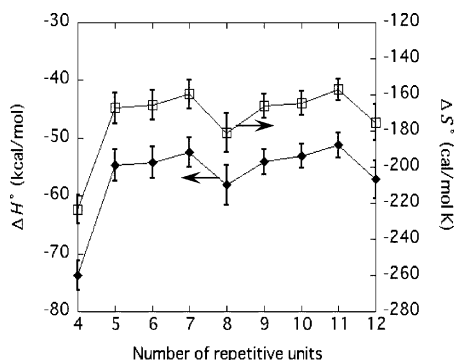


Figure 5. ΔH° and ΔS° values of the antiparallel G-quadruplexes of the (TTTTGGGG)_{*n*=4–12} in the presence of 100 mM Na⁺. ♦ and □ indicate ΔH° and ΔS° values, respectively.

mM Na⁺. The ΔH° value for (TTTTGGGG)₈ (−58.9 kcal/mol) is lower than that of (TTTTGGGG)₇ (−52.4 kcal/mol). Similarly, the ΔS° value for (TTTTGGGG)₈ (−181 cal/mol·K) is also lower than that for (TTTTGGGG)₇ (−159 cal/mol·K). A similar tendency was observed in the ΔH° and ΔS° values for (TTTTGGGG)₁₂ and (TTTTGGGG)₁₁. These results indicate that (TTTTGGGG)₈ can fold into two G-quadruplex units (i.e., each G-quadruplex structure is composed of four repeats), but that (TTTTGGGG)₇ can form only one G-quadruplex unit. Thus, it is reasonable that the ΔH° and ΔS° values for (TTTTGGGG)₈ were lower than those for (TTTTGGGG)₇ because the two G-quadruplex units of the former form more stacking and hydrogen-bond interactions and coordinate more cations. This also accounts for the tendency of the ΔH° and ΔS° values for (TTTTGGGG)₁₂, which forms three G-quadruplex units, to be lower than those of (TTTTGGGG)₁₁.

The ΔH° and ΔS° values for (TTTTGGGG)₈ were lower than those for (TTTTGGGG)₉. The reason for this was unclear

Table 1. Free Energy Change at 37 °C (ΔG°_{37}) of Intramolecular G-Quadruplex Formation of (TTTTGGGG)_{*n*=4–12} in the Presence of Na⁺

N	ΔG°_{37} (kcal/mol)	N	ΔG°_{37} (kcal/mol)
4	−4.34 ± 0.14	9	−2.67 ± 0.10
5	−2.84 ± 0.13	10	−2.54 ± 0.11
6	−2.91 ± 0.12	11	−2.53 ± 0.18
7	−2.92 ± 0.13	12	−2.50 ± 0.11
8	−2.93 ± 0.17		

because the number of G-quadruplex units would be the same. Notably, the G-quadruplex of (TTTTGGGG)₉ has one flanking sequence (free repeat) but (TTTTGGGG)₈ does not, and Guo et al. previously reported that the elongation flanking sequence thymidines at the 5′-end of the TTTTGGGG sequence significantly destabilize the G-quadruplex.⁴² Thus, flanking sequences destabilize the G-quadruplex structure of long telomeric DNAs, which can explain why the ΔH° and ΔS° values for (TTTTGGGG)₉ were larger than those for (TTTTGGGG)₈. Similarly this can explain why the values for (TTTTGGGG)₅ were lower than those for (TTTTGGGG)₄.

On the other hand, the ΔG°_{37} values listed in Table 1 changed little as the repeat number increased from 5 to 12, indicating that the stability of G-quadruplexes folded by longer *Oxytricha* telomeric DNAs ($n = 5–12$) is mostly independent of sequence length; however, the difference in ΔG°_{37} for G-quadruplex formation between (TTTTGGGG)₄ and (TTTTGGGG)₅ is relatively large (1.5 kcal/mol). Moreover, the difference between the ΔH° values for (TTTTGGGG)₄ and (TTTTGGGG)₅ shows that the lower stability of (TTTTGGGG)₅ is due to the unfavorable enthalpy change of the G-quadruplex of (TTTTGGGG)₅. These results suggest that disturbance of the hydrogen bonds by the flanking sequence and/or association of fewer cation or water molecules contributes significantly to the stability of G-quadruplexes with shorter sequences.

Three conclusions can be drawn from the thermodynamic properties of long *Oxytricha* telomeric DNAs: (1) the intramolecular G-quadruplex structure is more stable than the intermolecular G-quadruplex structure, (2) the stability of the intramolecular G-quadruplex formed by longer sequences is mostly independent of the sequence length, and (3) the free flanking sequences can affect the thermodynamics of G-quadruplex formation.

Thermodynamic Properties of Long Human Telomeric DNAs. We also studied the thermodynamic properties of long human telomeric DNAs in the presence of K⁺ or Na⁺ by melting curve analysis. Figure 6A shows the annealing and melting curves of (TTAGGG)₄ in a buffer containing 100 mM KCl and 50 mM Tris-HCl (pH 7.0). The single sigmoid melting curve in Figure 6A indicates that the antiparallel and parallel G-quadruplexes observed in the structural study (Figure 3B) have very similar thermal stabilities. Moreover, the melting and annealing curves did not show hystereses, suggesting a two-state transition of the G-quadruplex formation in the presence of K⁺. Figure 6B shows that the T_m values were independent of the DNA concentration in the presence of K⁺. Similarly, the annealing and melting curves for (TTAGGG)₄ also showed a single sigmoid shape in the buffer containing 100 mM NaCl and 50 mM Tris-HCl (pH 7.0), and a hysteresis was not

(42) Guo, Q.; Lu, M.; Kallenbach, N. R. *Biochemistry* **1993**, *32*, 3596–3603.

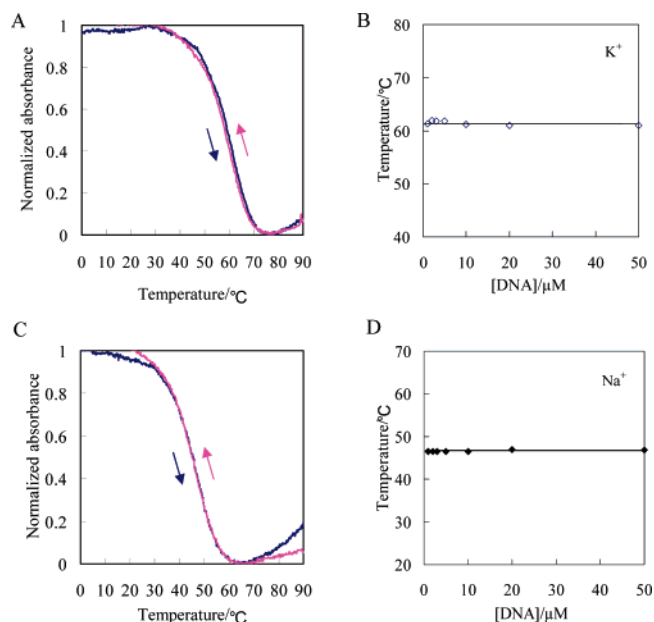


Figure 6. (A) Normalized thermal annealing (pink) and melting (blue) profile recorded at 295 nm for (TTAGGG)₄ in 50 mM Tris-HCl (pH 7.0) containing 100 mM K⁺. (B) Plot of T_m vs concentration of (TTAGGG)₄ (1–50 μM strand concentration) in 50 mM Tris-HCl (pH 7.0) containing 100 mM K⁺. (C) Normalized thermal annealing (pink) and melting (blue) profile recorded at 295 nm for (TTAGGG)₄ in 50 mM Tris-HCl (pH 7.0) containing 100 mM Na⁺. (D) Plot of T_m vs concentration of (TTAGGG)₄ (1–50 μM strand concentration) in 50 mM Tris-HCl (pH 7.0) containing 100 mM Na⁺.

observed, suggesting a two-state transition for the G-quadruplex in the presence of Na⁺ (Figure 6C). Moreover, the T_m values were independent of the DNA concentration in the presence of Na⁺ (Figure 6D). The other longer human telomeric DNAs ($n = 5–12$) have similar behaviors (see Figure S2 for the melting curves and the plot of T_m values versus concentration of human telomeric DNA in the presence of K⁺ and Na⁺). These results confirm that the human telomeric DNAs fold into intramolecular G-quadruplexes in the presence of K⁺ or Na⁺, which agrees with the structural analysis (Figure 3).

Because formation of the intramolecular G-quadruplex in the presence of K⁺ and Na⁺ is in a two-state transition between the single-stranded random coil and G-quadruplex, we estimated ΔH° , ΔS° , and ΔG°_{37} for G-quadruplex formation in the presence of K⁺ or Na⁺ by fitting melting curves to the theoretical equation for an intramolecular association.²⁸ Like the *Oxytricha* telomeric DNAs, the sequences of (TTAGGG) _{$n=4,8,12$} had ΔH° values distinctly lower than their neighboring sequences in the presence of K⁺ or Na⁺ (Figure 7). For example, in the presence of K⁺, the ΔH° and ΔS° values for (TTAGGG)₈ were lower than those for (TTAGGG)₇ and (TTAGGG)₉. These results suggest that, regardless of the species, telomeric sequences whose repeat number is a multiple of four are more ordered than other sequences. Interestingly, in the presence of K⁺ or Na⁺, the ΔH° and ΔS° values tended to decrease as the repeat number increased from 5 to 7 or from 9 to 11. This suggests that there are more interactions and higher rigidity as the sequence length increases. A possible reason for this is that the flanking sequences of human antiparallel G-quadruplexes can form Watson–Crick T–A base pairs, leading to reduced ΔH° and ΔS° values. Macaya et al. found that a

duplex tail greatly stabilizes G-quadruplex structures.⁴³ It is reasonable that the ΔH° value increased in *Oxytricha* telomeric DNAs when n was raised from 5 to 7 or from 9 to 11 (Figure 5) because its flanking sequence contains only T and G, which cannot form Watson–Crick base pairs. Thus, the sequence of the flanking tail also affects the thermodynamic properties of the structures formed by long human telomeric DNAs.

Moreover, on the basis of ΔG°_{37} values (Table 2), we found that the intramolecular G-quadruplexes formed by the human telomeric DNAs in the presence of K⁺ are more stable than those formed in the presence of Na⁺. This agrees with the previous observation that K⁺ is more effective at stabilizing G-quadruplexes of short telomeric DNAs than other monovalent cations.^{44–46} Like *Oxytricha* telomeric DNAs, the sequence length has little effect on the thermal stability of the intramolecular G-quadruplex formed by the longer human telomeric DNAs ($n = 5–12$). The differences in the ΔG°_{37} values for (TTAGGG)₄ and (TTAGGG)₅ are also relatively large in the presence of K⁺ and Na⁺ (1.26 and 0.55 kcal/mol, respectively) compared with the differences between longer sequences. This appears to be due to the same reasons described for the *Oxytricha* telomeric DNAs.

Possible Structures of the Long *Oxytricha* and Human Telomeric DNAs and Their Biological Significance. The results of the current study revealed the possible structural arrangement of G-quadruplexes formed by long telomeric DNAs that are long enough to form more than one G-quadruplex unit. The ΔH° and ΔS° values of (TTTTGGGG) _{$n=4,8,12$} and (TTAGGG) _{$n=4,8,12$} generally increase with the sequence length (Figures 5 and 7). These parameters suggest that the two or three G-quadruplex units do not interact because interactions such as stacking and hydrogen bonding should decrease the ΔH° and ΔS° values. Therefore, it appears that long telomeric DNAs tend to arrange as distinct G-quadruplex units joined by a TTTT linker (*Oxytricha*) or TTA linker (human), resembling beads on a string, and that the G-quadruplexes are not generated by stacking interactions (Figure 1C). Overall, the bead-on-a-string structure should be similar for long telomeric DNAs irrespective of the specific components. Figure 8 shows the possible structures of long *Oxytricha* and human telomeric DNAs based on the G-quadruplex conformations of short *Oxytricha*⁴⁷ and human^{48,49} telomeric DNAs, wherein the conformation of the G-quadruplex units in a bead-on-a-string may be different from each other.

The bead-on-a-string structure is more reasonable than the stacking structure for various biological roles of the telomeric DNAs. For example, during meiosis, telomeric DNAs are not lost all at once but rather are shortened step by step.⁵⁰ If the telomeres adopt the stacking structure, the entire structure must unfold before each round of meiosis and fold into a new stacking structure after meiosis, which seems unreasonable from the

(43) Macaya, R. F.; Waldron, J. A.; Beutel, B. A.; Gao, H.; Joesten, M. E.; Yang, M.; Patel, R.; Bertelsen, A. H.; Cook, A. F. *Biochemistry* **1995**, *34*, 4478–4492.

(44) Hardin, C. C.; Henderson, E.; Watson, T.; Prosser, J. K. *Biochemistry* **1991**, *30*, 4460–4472.

(45) Sen, D.; Gilbert, W. *Biochemistry* **1992**, *31*, 65–70.

(46) Sen, D.; Gilbert, W. *Nature* **1990**, *344*, 410–414.

(47) Smith, F. W.; Schultze, P.; Feigon, J. *Structure* **1995**, *3*, 997–1008.

(48) Marathias, V. M.; Bolton, P. H. *Biochemistry* **1999**, *38*, 4355–4364.

(49) He, Y.; Neumann, R. D.; Panyutin, I. G. *Nucleic Acid Res.* **2004**, *32*, 5359–5367.

(50) Bryan, T. M.; Cech, T. R. *Curr. Opin. Cell Biol.* **1999**, *11*, 318–324.

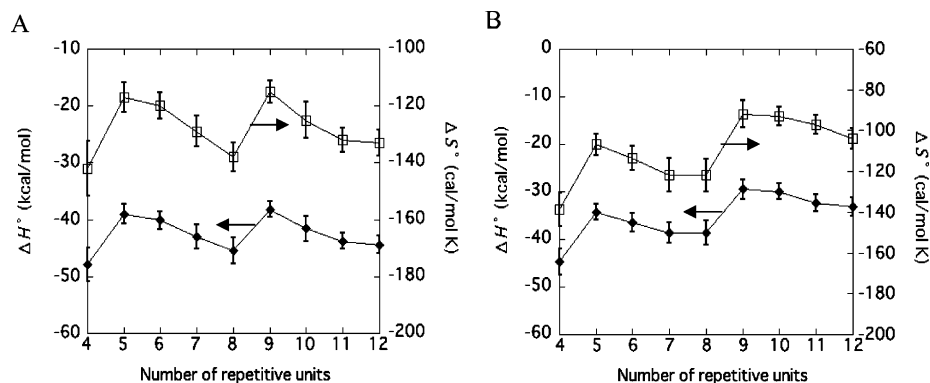


Figure 7. (A) ΔH° and ΔS° values of the parallel and antiparallel G-quadruplexes of the $(TTAGGG)_{n=4-12}$ in the presence of 100 mM K^+ . (B) ΔH° and ΔS° values of the antiparallel G-quadruplexes of the $(TTAGGG)_{n=4-12}$ in the presence of 100 mM Na^+ . \blacklozenge and \square indicate ΔH° and ΔS° values, respectively.

Table 2. Free Energy Change at 37 °C (ΔG°_{37}) of Intramolecular G-Quadruplex Formation of $(TTAGGG)_{n=4-12}$

n	ΔG°_{37} (kcal/mol)	
	K^+	Na^+
4	-3.83 ± 0.14	-1.63 ± 0.09
5	-2.57 ± 0.11	-1.08 ± 0.08
6	-2.70 ± 0.12	-1.13 ± 0.10
7	-2.92 ± 0.15	-1.38 ± 0.07
8	-3.02 ± 0.17	-1.32 ± 0.09
9	-2.58 ± 0.09	-1.06 ± 0.05
10	-2.83 ± 0.09	-1.11 ± 0.05
11	-2.98 ± 0.10	-1.22 ± 0.07
12	-3.16 ± 0.11	-1.08 ± 0.10

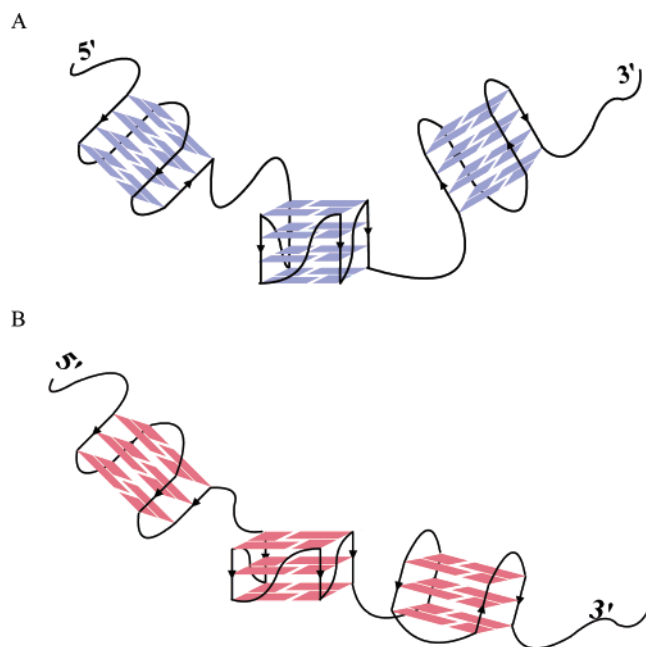


Figure 8. Schematic diagrams of the bead-on-a-string structures of G-quadruplexes formed by (A) long *Oxytricha* and (B) human telomeric DNAs.

viewpoints of energy cost and the kinetics of G-quadruplexes.⁵¹ On the other hand, if the telomeres adopt the bead-on-a-string structure, the telomeres can be shortened step by step without unfolding the entire G-quadruplex structure. On the basis of X-ray crystallographic analysis of short human telomeric DNAs, Parkinson et al. also proposed a similar G-quadruplex structure in which every four repeats fold into a parallel propeller

G-quadruplex unit,²⁰ although this is somewhat different from our model; there is a stacking interaction between every two G-quadruplex units in their model, whereas our data indicated that the stacking interactions between G-quadruplex units are unfavorable under the conditions examined here. Thus, the bead-on-a-string structure proposed here may be more representative of the structure of long telomeric DNAs in solution.

Conclusion

The present results revealed the behaviors of long telomeric DNAs in solution. First, the long *Oxytricha* telomeric DNAs are more polymorphic than human telomeric DNAs, indicating that the sequence plays an important role in G-quadruplex formation as reported for short telomeric DNAs. Moreover, the ionic conditions greatly affect G-quadruplex conformation; for example, long telomeric DNAs fold into antiparallel G-quadruplexes in the presence of Na^+ , whereas they fold into a mixture of parallel and antiparallel G-quadruplexes in the presence of K^+ . These results are generally consistent with the previous results for short telomeric DNAs. Second, the measurements of ΔH° and ΔS° revealed that the G-quadruplex structure is affected by the flanking sequences. This phenomenon was also reported for short telomeric DNAs. Thus, short and long telomeric DNAs have common properties. Last and most importantly, our thermodynamic results demonstrate for the first time that the most reasonable arrangement of the long telomeric DNAs is a bead-on-a-string structure in which the individual G-quadruplex units adopt the G-quadruplex structure. This may represent an important feature of long telomeric DNAs and may help clarify the mechanism of telomere shortening. Together, these findings should help advance telomere science and aid in the development of drugs and ligands targeting telomeric DNAs and telomerase.

Acknowledgment. This work was supported in part by Grants-in-Aid for Scientific Research and for the Academic Frontier Project (2004-2009) from the Ministry of Education, Culture, Sports, Science and Technology, Japan.

Supporting Information Available: Figure S1, the melting curves and the plot of T_m values versus concentration of *Oxytricha* telomeric DNAs in the presence of K^+ and Na^+ ; and Figure S2, the melting curves and the plot of T_m values versus concentration of human telomeric DNAs in the presence of K^+ and Na^+ . This material is available free of charge via the Internet at <http://pubs.acs.org>.

(51) Phan, A. T.; Mergny, J. L. *Nucleic Acids Res.* **2002**, *30*, 4618–4625.